A damped oscillator imposes temporal order on posterior gap gene expression in *Drosophila*

Berta Verd[a,b,c,1], Erik Clark[d], Karl R. Wotton[a,b,2], Hilde Janssens[a,b], Eva Jiménez-Guri[a,b,2], Anton Crombach[a,b,e,3], and Johannes Jaeger[a,b,c,e]

[a]EMBL/CRG Systems Biology Research Unit, Centre for Genomic Regulation (CRG), The Barcelona Institute of Science and Technology, Dr. Aiguader 88, 08003 Barcelona, Spain
[b]Universitat Pompeu Fabra (UPF), Barcelona, Spain
[c]KLI Klosterneuburg, Austria
[d]Department of Zoology, University of Cambridge, Cambridge, UK
[e] Wissenschaftskolleg zu Berlin, Germany

January 13, 2017

Abstract

Insects determine their body segments in two different ways. Short-germband insects, such as the flour beetle *Tribolium castaneum*, use a molecular clock to establish segments sequentially. In contrast, long-germband insects, such as the vinegar fly *Drosophila melanogaster*, determine all segments simultaneously through a hierarchical cascade of gene regulation. Gap genes constitute the first layer of the *Drosophila* segmentation gene hierarchy, downstream of maternal gradients. We use data-driven modelling and phase space analysis to show that shifting gap domains in the posterior half of the *Drosophila* embryo are an emergent property of a robust damped oscillator mechanism. Simulations and experiments show that maternal Caudal (Cad) levels influence the rate at which posterior gap domains shift, reminiscent of how Cad regulates the frequency of the *Tribolium* molecular clock. Our evidence indicates that the regulatory dynamics underlying long- and short-germband segmentation are much more similar than previously thought. Understanding such similarities may help explain why the short- to long-germband transition occurred convergently multiple times during the radiation of the holometabolan insects.

The segmented body plan of insects is established by two seemingly very different modes of development [60, 16, 59, 38]. Long-germband insects, such as the vinegar fly *Drosophila melanogaster*, determine their segments more or

less simultaneously during the blastoderm stage, before the onset of gastrulation [1, 28]. The segmental pattern is set up by subdivision of the embryo into different territories, prior to any growth or tissue rearrangements. Short-germband insects, such as the flour beetle *Tribolium castaneum*, determine most of their segments after gastrulation, with segments being patterned sequentially from a posterior segment addition zone. This process involves tissue growth or rearrangements as well as dynamic travelling waves of gene expression driven by a molecular clock mechanism [61, 18, 19, 46]. The available evidence strongly suggests that the short-germband mode of segment determination is ancestral, while the long-germband mode is evolutionarily derived [60, 16, 37].

Although the ancestor of holometabolan (metamorphosing) insects may have exhibited some features of long-germband segment determination [63], it is clear that convergent transitions between the two modes have occurred frequently during evolution [16, 37, 53]. Long-germband segment determination can be found scattered over all four major holometabolous insect orders (Hymenoptera, Coleoptera, Lepidoptera, and Diptera). Furthermore, there has been at least one reversion from long- to short-germband segment determination in polyembryonic wasps [66]. This suggests that despite the apparent differences between the two segmentation modes, it seems relatively easy to evolve one from the other. Why this is so, and how the transition is achieved, remains unknown.

In this paper, we provide evidence suggesting that the patterning dynamics of long- and short-germband segmentation are much more similar than previously thought. Specifically, we demonstrate that shifting domains of segmentation gene expression in the posterior of the *D. melanogaster* embryo can be explained by a damped oscillator mechanism, dynamically very similar to the clock-like mechanism underlying short-germband segment determination. We achieve this through analysis of a quantitative, data-driven gene circuit model of the gap network in *D. melanogaster*. The gap gene system constitutes the top-most hierarchical layer of the segmentation gene cascade [28]. Gap genes *hunchback (hb)*, *Krüppel (Kr)*, *giant (gt)*, and *knirps (kni)* are activated through gradients formed by the products of maternal co-ordinate genes *bicoid (bcd)* and *caudal (cad)*. Gap genes are transiently expressed during the blastoderm stage in broad overlapping domains along the antero-posterior (A–P) axis of the embryo (Fig. 1A). They play an important role regulating periodic pair-rule gene expression. Pair-rule genes, in turn, establish the precise pre-pattern of the segment-polarity genes, whose activities govern the morphological formation of body segments later in development, after gastrulation has occurred.

Our aim is to go beyond the static reconstruction of network structure, to fully and explicitly understand the regulatory dynamics of the patterning process [31, 32]. To achieve this aim, we use the powerful tools of dynamical systems theory—especially the geometrical analysis of *phase* (or *state*) space [64]—to characterise the patterning capacity of the gap gene network (technical terms in italics are explained in the glossary, in the Supplementary Information). We study the complex regulatory mechanisms underlying gap gene expression in terms of the number, type, and arrangement of *attractors* and their associated *basins of attraction*, which define the *phase portrait*. The geometry of the phase

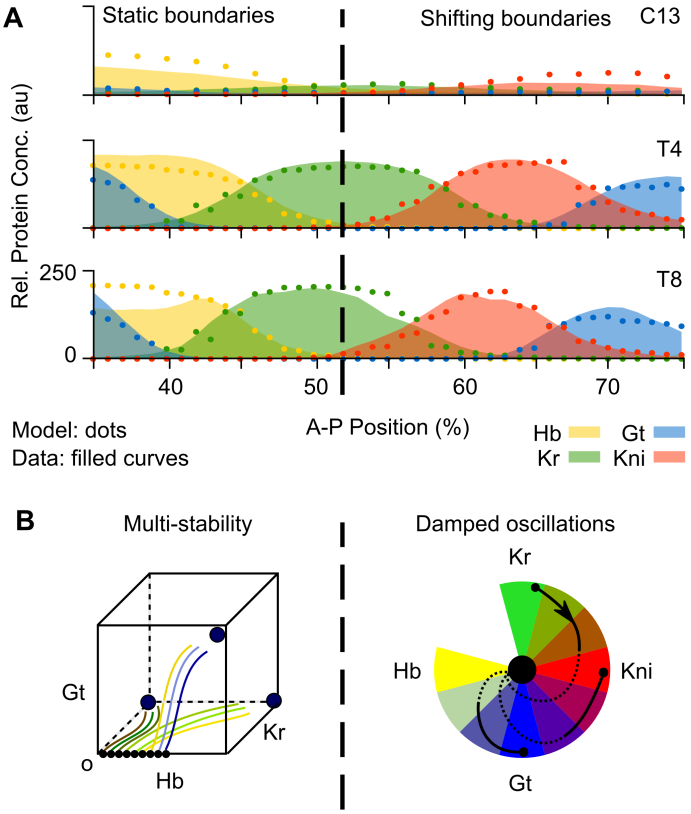

Figure 1: **Dynamics of gap gene pattern formation in *D. melanogaster*.** **(A)** Gap protein expression data (coloured areas) and model output (dots), shown at cleavage cycles C13 and C14A (time classes T4 and T8). Hb in yellow, Kr in green, Kni in red, Gt in blue (see key). X-axes: % A–P position (where 0% is the anterior pole); Y-axes: relative protein concentration (in arbitrary units, au). Dashed vertical line indicates bifurcation boundary between static and shifting gap domain borders (at 52% A–P position). **(B)** Dynamic regimes governing gap gene expression in the anterior versus the posterior of the embryo. Static anterior boundaries are set by attractors in a multi-stable regime, as shown in the stylized phase portrait on the left; shifting posterior boundaries are driven by a damped oscillator implemented by a monostable spiral sink (right). Colour wheel with black trajectories represents ordered dynamics of gap gene expression driven by the damped oscillator (see text for details).

portrait in turn determines the *flow* of the system. This flow consists of individual *trajectories* that describe how the *system state* changes over time given some specific *initial conditions*. In our gap gene circuit model, *initial conditions* are given by the maternal Hb gradient, *boundary conditions* by the maternal Bcd and Cad gradients, and the *state variables* consist of the concentrations of regulators Hb, Kr, Kni, and Gt. Different configurations of phase space will give rise to differently shaped trajectories and, thus, to different gap gene regulatory dynamics.

The power of analogy between phase space and its features, and developmental mechanisms has long been recognised and exploited. In their original clock and wavefront model, Cooke and Zeeman [9] characterise cells involved in somitogenesis in the pre-somitic mesoderm as "oscillators with respect to an unknown clock or *limit cycle* in the embryo". More recently, geometrical analysis of phase space continues to be successfully used to study somitogenesis [48] and other developmental processes such as vulval development or antero-posterior patterning by the Hox genes [10, 20] including the robust (canalized) patterning dynamics of gap genes [41, 40, 70, 25]. To make the problem tractable, these analyses were performed in a simplified context. In the context of *Drosophila* segmentation, models were used with a static Bcd gradient and Cad dynamics frozen at a particular time point during the late blastoderm stage [34, 29, 41, 40, 25]. This renders the system *autonomous*, meaning that model parameters—and therefore phase space geometry—remain constant over time.

However, the maternal gradients of Bcd and Cad change and decay on the same time scale as gap gene expression [67]. Taking this time-dependence of maternal regulatory inputs into account leads to a *non-autonomous* system, in which model parameters are allowed to change over time. This causes the geometry of phase space to become time-variable: the number, type, and arrangement of attractors and their basins change from one time point to the next. *Bifurcations*—the creation or annihilation of attractors—may occur over time, and trajectories may cross from one basin of attraction to another. All of this makes non-autonomous analysis highly non-trivial. We have developed a novel methodology to characterise transient dynamics in non-autonomous models [71]. It uses *instantaneous phase portraits* [8, 72] to capture the time-variable geometry of phase space and its influence on system trajectories.

By fitting models to quantitative spatio-temporal gene expression data, we have obtained a diffusion-less, fully non-autonomous gap gene circuit featuring realistic temporal dynamics of both Bcd and Cad [2, 72] (see Materials and Methods, and Supplementary Information). This model surpasses previous models, taking accuracy and realism to levels that cannot be reached using simpler formulations. Moreover, the model has been extensively validated against experimental data [34, 29, 41, 40, 2, 72], and represents a regulatory network structure that is consistent with genetic and molecular evidence [28].

We have performed a detailed and systematic phase space analysis of this non-autonomous gap gene circuit. It allowed us to identify and characterise different *dynamic regimes* and explicitly time-dependent aspects of gap gene

regulation [72]. In the anterior of the embryo, where boundary positions remain stationary over time, gap gene expression dynamics are governed by a multistable regime (Fig. 1B). This is consistent with earlier work [40], indicating that modelling results are consistent across analyses. Here, we focus on the regulatory mechanism underlying patterning dynamics in the posterior of the embryo, which differs between autonomous and non-autonomous analyses. Posterior gap domains shift anteriorly over time [34, 67]. Autonomous analysis suggested that these shifts are driven by a feature of phase space called an *unstable manifold* [40], while our non-autonomous analysis reveals that they are governed by a monostable *spiral sink*, which shapes the trajectories (Fig. 1B). The presence of a spiral sink implies that a *damped oscillator* mechanism is driving gap domain shifts in our model [64]. In this paper, we present a detailed analysis of this oscillator mechanism and discuss its implications for pattern formation and the evolution of the gap gene system. Our results suggest that long-germband and short-germband modes of segmentation both involve oscillatory regimes in the posterior region of the embryo that generate posterior to anterior waves of gene expression. Characterising and understanding these unexpected similarities provides a necessary first step towards a mechanistic explanation for the surprisingly frequent occurrence of convergent transitions between the two modes of segment determination during holometabolan insect evolution.

Results

Gap domain shifts are an emergent property of a damped oscillator

Gap domain boundaries posterior to 52% A–P position shift anteriorly over time (Fig. 1A) [34, 67]. These domain shifts cannot be explained by nuclear movements [35], nor do they require diffusion or transport of gap gene products between nuclei [34, 41, 40, 72]. Instead, gap domain shifts are kinematic, caused by an ordered temporal succession of gene expression in each nucleus, which produces apparent wave-like movements in space [34, 40]. This is illustrated in Fig. 2A. Each nucleus starts with a different initial concentration of maternal Hb, which leads to the expression of different zygotic gap genes: *Kr* in the central region of the embryo, or *kni* further posterior. Nuclei then proceed through a stereotypical temporal progression where *Kr* expression is followed by *kni* (*e. g.* nucleus at 59%), *kni* by *gt* (nucleus at 69%) and, finally, *gt* by *hb* (nuclei posterior of 75%; not shown). No nucleus goes through the expression of all four trunk gap genes over the course of the blastoderm stage and each nucleus goes through a different partial sequence within this progression, according to its initial conditions. This coordinated dynamic behaviour is what we need to explain in order to understand the regulatory mechanism underlying gap domain shifts.

To do this we carried out a systematic characterisation of dynamical regimes in a non-autonomous gap gene circuit [72]. This analysis reveals that phase por-

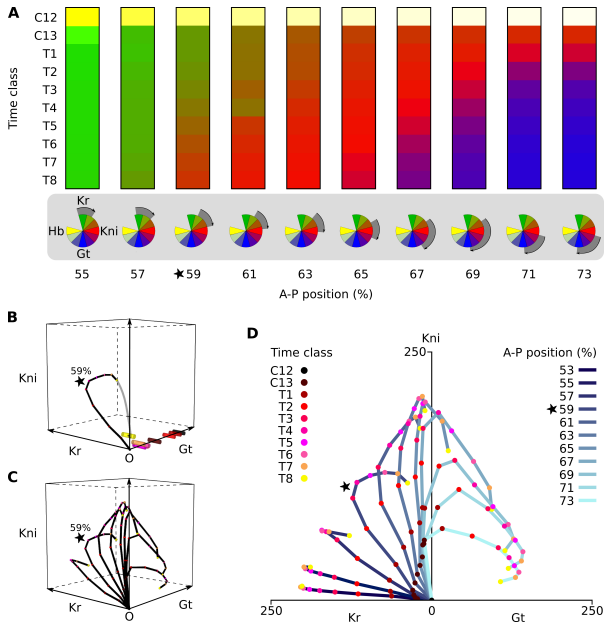

Figure 2: **A damped oscillator governs posterior gap gene patterning in *D. melanogaster*. (A)** Kinematic gap domain shifts and temporal order of gene expression. Temporal dynamics of gap gene expression in posterior nuclei between 55% and 73% A–P position shown as columns. Developmental time proceeds down the Y-axis, covering cleavage cycles C13 and C14A (time classes T1–8). C12 indicates initial conditions: maternally provided Hb concentrations indicated by yellow shading at the top of each column. Kr concentration is shown in shades of green, Kni in red, and Gt in blue. The kinematic anterior shift of the Kni domain (in red) is clearly visible. Colour-wheels (at the bottom of the columns) represent ordered succession of gap gene gene expression imposed by the damped oscillator mechanism. Black arrows indicate the section (phase range) of the clock period that the oscillator traverses in each nucleus over the duration of the blastoderm stage. The position of each arrow depends on the initial Hb concentration in that nucleus. **(B)** Three-dimensional projection of the time-variable phase portrait for the nucleus at 59%A–P position. Axes represent Kr, Kni, and Gt protein concentrations. Spiral sinks are represented by cylinders, colour-coded to show the associated developmental time point (see key). The trajectory of the system during C13 and C14A is shown in black, coloured points marking its progress through time. Asymptotic convergence of the trajectory (after the blastoderm stage has ended) is shown in grey. **(C)** Trajectories for every other nucleus between 57 and 71%A–P position. Projection, axes, and time points as in (B). **(D)** Trajectories for the nuclei between 53 and 73%A–P position are represented unfolded onto the Kr-Kni and Gt-Kni planes. A–P position of nuclei is given by the shade of blue of the trajectory: lighter coloured trajectories correspond to more posterior nuclei (see key). Time points as in (B). The star marks the nucleus at 59% A–P position. See Materials and Methods for time classes, and main text for further details.

traits of nuclei posterior to 52% A–P position are monostable throughout the blastoderm stage (see, for example, Fig. 2B). Given enough time, all trajectories would approach the only attractor present, which at T8 is located at high *hb* levels (Fig. 2B, yellow cylinder). Due to the non-autonomy of the system, this attractor moves across phase space over developmental time. However, this movement is not the most important factor determining the shape of trajectories. Due to the limited duration of the blastoderm stage, the system always remains far from steady state, and posterior gap gene expression dynamics are shaped by the geometry of transient trajectories, relatively independently of the precise position of the attractor. Because the moving attractor positions of all posterior nuclei are similar to those shown for the nucleus at 59% A–P (Fig. 2B), we are able to plot the trajectories of the different nuclei onto the same projection of phase space (Fig. 2C). Posterior nuclei cycle through build-up of Kr, then Kni, then Gt protein, with their initial conditions determining where in this sequence they begin. It is evident from the plots in Fig. 2B and C that the ordered succession of gap gene expression is a consequence of the rotational (spiral-shaped) geometry of the trajectories.

Eigenvalue analysis reveals that the monostable steady state in posterior nuclei is a special type of point attractor: a *spiral sink*, or *focus* [64, 72]. Trajectories do not approach a sink in a straight line, but spiral inward instead. This contributes to the curved rotational geometry of the trajectories shown in Fig. 2B and C. From the theory of dynamical systems, we know that spiral sinks are the hallmark of damped oscillations [64]. Given that spiral sinks are the only steady states present in the monostable phase portraits of posterior nuclei, we conclude that posterior gap gene expression dynamics in our model are driven by a damped oscillator mechanism. This damped oscillator mechanism imposes the observed temporal order of gap gene expression (Fig. 2A). Temporal order is a natural consequence of oscillatory mechanisms, one obvious example being the stereotypical succession of cyclin gene expression driven by the cell cycle oscillator [44, 47]. This is not a general property of unstable manifolds (found to drive gap domain shifts in previous autonomous analyses [40, 70, 25]). In this sense, our damped oscillator mechanism provides a more straightforward and intuitive explanation of gap domain shifts and constitutes an important conceptual advance over previous characterisations.

Yet, the proposed oscillatory mechanism can appear counter-intuitive. It never produces any repeating cyclical behaviour, such as the periodic waves of gene expression involved in short-germband segmentation in insects [61, 18, 19] and other arthropods [6, 4], or vertebrate somitogenesis [50, 48]. Still, it fully satisfies the definition of an oscillator. Each nucleus runs through a different range of phases within a given time range (see color-wheel diagrams in Fig. 2A), like clocks that never complete the hour. Arranged properly across space, such shifted partial phase oscillations create the observed kinematic waves of gene expression. In this sense, the dynamics of shifting gap domains in the *D. melanogaster* blastoderm and travelling waves of gene expression in short-germband embryos are equivalent, since they are both an emergent property of an underlying oscillatory regulatory mechanism.

Canalising properties of the gap gene damped oscillator

In principle, domain shifts are not strictly necessary for subdividing an embryo into separate gene expression territories. Wolpert's French Flag paradigm for positional information, for example, works without any dynamic patterning downstream of the morphogen gradient [76, 77]. This raises the question of why such shifts occur and what, if anything, they contribute to pattern formation. One suggestion is that feedback-driven shifts lead to more robust patterning than a strictly feed-forward regulatory mechanism such as the French Flag [33, 30]. This is supported by the fact that the unstable manifold found in autonomous analyses [40] has canalising properties: as time progresses, it attracts trajectories coming from different initial conditions into an increasingly small and localised sub-volume of phase space. This desensitizes the system to variation in maternal gradient concentrations [41]. Based on these insights, we asked whether our damped oscillator mechanism exhibits similar canalising behaviour, ensuring robust gap gene patterning.

A closer examination of the spiral trajectories in Fig. 2C reveals that they are largely confined to two specific sub-planes in phase space. Specifically, they tend to avoid regions of simultaneously high Gt and Kr, allowing us to "unfold" the three-dimensional volume of Kr-Kni-Gt space into two juxtaposed planes representing Kr-Kni and Kni-Gt concentrations (Fig. 2D). This projection highlights how trajectories spend variable amounts of time in the Kr-Kni plane before they transition onto the Kni-Gt plane.

In order to investigate the canalising properties of our damped oscillator mechanism, we performed a numerical experiment, shown in Fig. 3A and B. We chose a set of regularly distributed initial conditions for our model that lie within the Kr-Gt plane (Fig. 3A) and used this set of initial conditions to simulate the nucleus at 59% A–P position with a fixed level of Kni (Fig.3B). These simulations illustrate how system trajectories converge to the Kr-Kni or Kni-Gt plane, avoiding regions of simultaneously high Kr and Gt concentrations. Convergence occurs rapidly and is already far advanced in early cleavage cycle 14A (Fig. 3B, time class T1). At later stages, convergence slows down but continues restricting trajectories to an increasingly small sub-volume of phase space (up to late cleavage cycle 14A, Fig. 3B, time class T8). This behaviour is robust with regard to varying levels of Kni (Supplementary Fig. 1). It demonstrates that the sub-volume of phase space in which trajectories are found becomes restricted long before a steady state is reached. This spatial restriction of transient trajectories is qualitatively equivalent to the canalising behaviour of the unstable manifold found in autonomous analyses [40].

It is straightforward to interpret the exclusion of trajectories from regions of simultaneous high Kr and high Gt in terms of regulatory interactions. There is a strong double-negative (and hence positive) feedback loop between *gt* and *Kr*, which is crucial for the mutually exclusive expression patterns of these genes [29, 28, 14]. In the context of our damped oscillator mechanism, this mutually exclusive feedback implies that the system must first transition from high Kr to high Kni/low Kr before it can initiate *gt* expression. This is exactly what

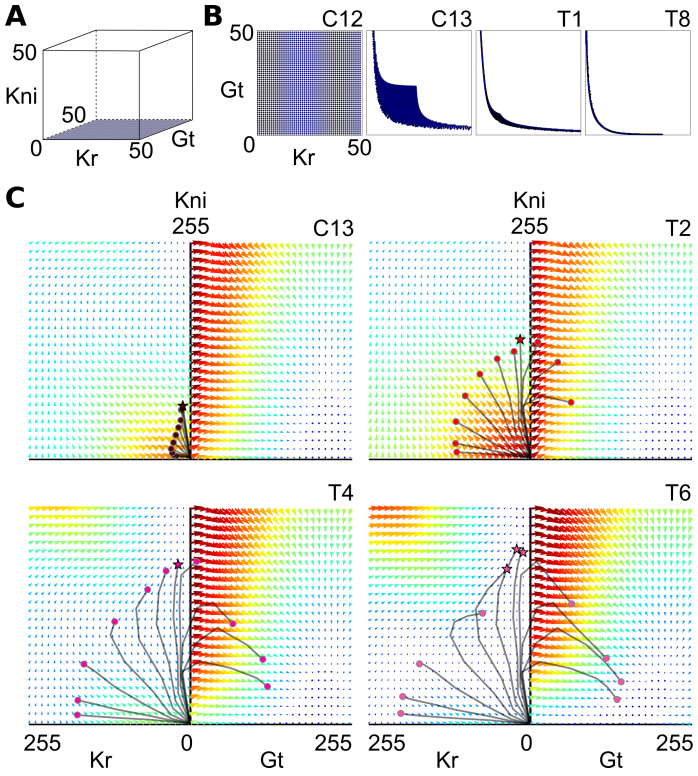

Figure 3: **Canalising properties and relaxation-like behaviour of the gap gene damped oscillator. (A, B)** Canalising properties: trajectories rapidly converge to planes in phase space. We simulate the non-autonomous diffusion-less circuit in the nucleus at 59% A–P position with Kni concentration fixed to zero and a set of initial conditions that are regularly distributed on the Kr-Gt plane. **(A)** Initial conditions shown in blue, embedded within the three-dimensional Kr-Kni-Gt space. **(B)** Two-dimensional projections of the Kr-Gt plane show converging system states as tiny blue dots at C12, C13, C14A-T1, and -T8. **(C)** Fast-slow dynamics in posterior nuclei are caused by relaxation-like behaviour. Unfolded, two-dimensional projections of the Kr-Kni and Kni-Gt planes are shown as in Fig. 2C at C13, C14A-T2, -T4, and -T6. Coloured arrows indicate magnitude and direction of flow: large red arrows represent strong flow, small blue arrows represent weak flow. Trajectories of posterior nuclei are superimposed on the flow (shown as black lines). Coloured circles at the end of trajectories indicate current state at each time point. Stars mark trajectories experiencing a positive Gt-component of the flow. See Materials and Methods for time classes, and main text for further details.

we observe (Fig. 2A), confirming that the damped oscillator in the posterior of the *D. melanogaster* embryo has canalising properties due to double-negative feedback between mutually exclusive gap genes.

Fast-slow dynamics through excitable relaxation-like oscillatory behaviour

How do spiral trajectories switch from one plane in phase space to another? Fig. 3C shows projections of the flow of our fully non-autonomous model onto the unfolded Kr-Kni and Kni-Gt planes, and maps trajectories and states of various posterior nuclei at different points in time onto this flow (see also Supplementary Fig. 2). These plots reveal drastic differences in flow velocity (magnitude) in different regions of phase space at different points in time. At early stages, close to the origin, we observe a fast initial increase in Kr and Kni concentrations (Fig. 3C, C13 and T2, red arrows at low Kr and Kni values). Nuclei whose trajectories remain on the Kr-Kni plane then show a dramatic slow-down. They either continue to gradually increase levels of Kr, or exhibit slow build-up of Kni combined with consequent decrease of Kr (due to repression by Kni; Fig. 3C, T4 and T6). As trajectories in different nuclei approach the border between the Kr-Kni and Kni-Gt planes, the Gt-component of the flow on the Kr-Kni plane becomes positive (trajectories marked by stars in Fig. 3C). This "lifts" the trajectory out of the Kr-Kni and into the Kni-Gt plane. In the border zone, the flow in the direction of Gt is high throughout the blastoderm stage (Fig. 3C), ensuring that the switch between planes occurs rapidly. Nuclei then again enter a zone of slower dynamics with a gradual build-up of Gt, combined with consequent decrease of Kni (due to repression by Gt; Fig. 3C, T4 and T6).

Thus, the flow of our model combines relatively slow straight stretches within a plane of phase space with rapid turns at the border between planes. Similar alternating fast-slow dynamics have been observed in autonomous models [70]. They influence the width of gap domains (through relatively stable periods of expressing a specific gap gene), and the sharpness of domain boundaries (through abrupt changes in gene expression at borders between planes). Such fast-slow dynamics are characteristic of *relaxation oscillations* [64]. A relaxation oscillator combines phases of gradual build-up in some of its state variables with rapid releases and changes of state, resulting from an irregularly-shaped *limit cycle* attractor. This suggests that the irregular geometries of spiralling transient trajectories in our model represent relaxation-like oscillatory dynamics that govern the shape and the shift rate of posterior gap domains.

The fast-slow dynamics we observe are typical for *excitable systems* (also called *excitable media*). Such systems exhibit dynamics governed by a single attractor with transient dynamics that can send trajectories on long excursions through phase space [64]. These conditions apply to both our fully non-autonomous system, as well as earlier autonomous analyses of the gap gene network [40, 70]. Excitability is not only important for shifting gap domains, but occurs in a vast range of natural non-linear systems, including the Belousov–Zhabotinsky chemical reaction and fruiting body aggregation in slime molds

[75, 45]. In this sense, gap domain shifts belong to a very common class of dynamic regulatory mechanisms, and insights from their study may apply in many other regulatory contexts.

Caudal regulates the velocity of gap domain shifts

In the short-germband beetle *T. castaneum*, an oscillator mechanism governs travelling waves of pair-rule gene expression [61, 18]. The frequency of these repeating waves is positively correlated with the level of Cad in the posterior of the embryo: the more Cad present, the faster the oscillations [19]. In *D. melanogaster*, changing concentrations of maternal morphogens influence the rate and extent of posterior gap domain shifts [78, 72]. Therefore, we asked whether Cad levels affect the damped oscillator mechanism regulating gap genes in *D. melanogaster* in a way that is analogous to its effect on pair-rule oscillations in *T. castaneum*.

We assessed the regulatory role of Cad by multiplying its concentration profile with different constant scaling factors and measuring the dynamics and extent of gap domain shifts in the resulting simulations (Fig. 4A). This reduces Cad levels throughout space and time without affecting the overall shape of its profile. Our results reveal that the Kr-Gt border interface (Fig. 4A, inset) starts out at the same position, regardless of Cad concentration (Fig. 4A, time class C13). This corroborates earlier analyses which suggest that maternal Hb (not Cad) is the main morphogen in the posterior of the embryo [65, 40, 28, 72]. Between C13 and T1, however, boundary positions diverge: gap domain shifts are slower for lower levels of Cad. From T1 onwards, as Cad levels decrease (and therefore the absolute magnitude of the difference in Cad levels amongst simulations), shift rates become more or less independent of Cad concentration and boundary positions move in parallel in different simulations for the rest of the blastoderm stage (Fig. 4A). This suggests that the rate of gap domain shifts—especially at early stages—depends on the concentration of Cad in the posterior of the embryo.

To test this model prediction, we quantified boundary shifts of Gt and Kni domains in mutant embryos lacking maternal *cad*. These mutants exhibit reduced levels of Cad protein throughout the blastoderm stage [39]. As predicted by our simulations, they show delayed shifts of the posterior Gt (Fig. 5A and B) and the abdominal Kni domains [78]. Taken together, our experimental and modelling evidence suggests that Cad positively regulates the velocity of gap domain shifts during early blastoderm stage in *D. melanogaster*, analogous to its positive correlation with pair-rule wave frequency in *T. castaneum*.

According to our model, Cad regulates the rate and extent of gap domain shifts by altering the fast-slow dynamics of the gap gene damped oscillator (Fig. 4B–D and Supplementary Fig. 3). While the direction of the flow remains largely constant across different levels of Cad, its magnitude changes significantly (Supplementary Fig. 3). Most importantly, the magnitude of the flow in the area of the Kr-Kni plane around the origin is strongly reduced at early stages (Fig. 4B–D, time class C12). At later stages, when wild-type Cad levels

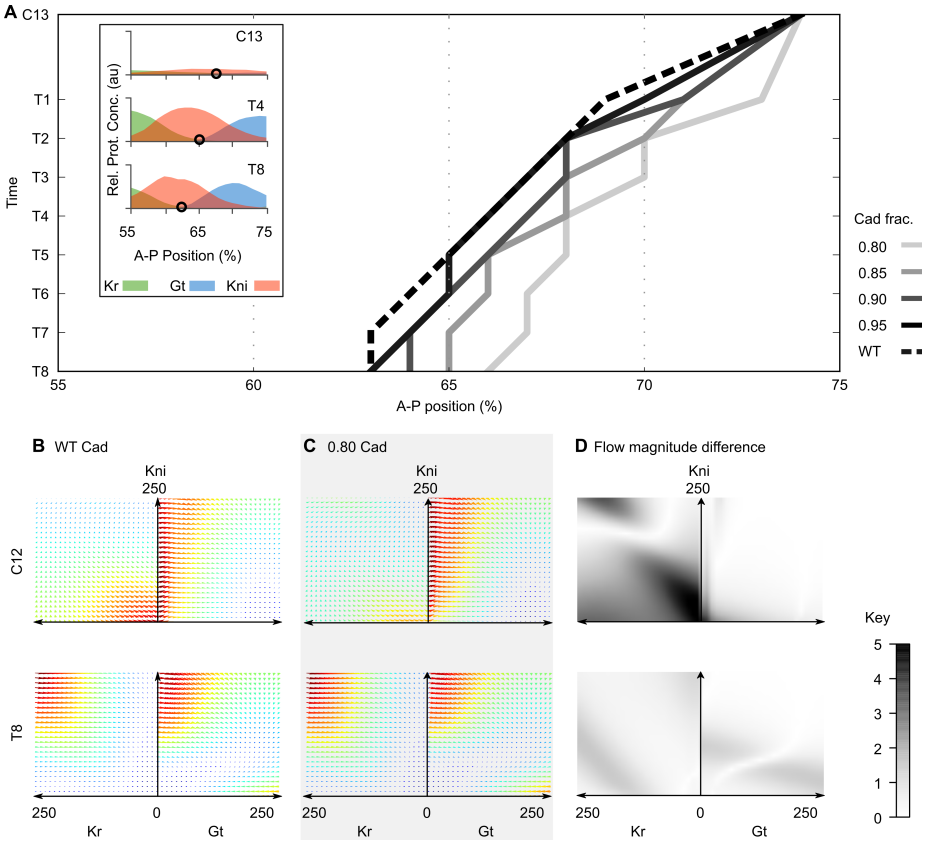

Figure 4: **Caudal levels modulate the initial velocity of gap domain shifts (A)** Space-time plot shows temporal shift of the Kr-Gt border interface in simulations with variable levels of Cad (see key and main text). Reduced levels of Cad imply slower shift between C13 and T1. Y-axis represents time (increasing downwards). Inset shows posterior gap gene expression data at time classes C13 and C14A-T4 and -T8. Black circles mark the Kr-Gt border interface. Y-axes show gap protein concentration in arbitrary units (au). X-axes represent % A–P position (where 0% is the anterior pole). **(B, C)** Stereotypical fast-slow dynamics for posterior nuclei simulated with a wild-type (WT) Cad profile and with a Cad profile multiplied by a factor of 0.8. Unfolded, two-dimensional projections of the Kr-Kni and Kni-Gt planes are shown as in Fig.3C at C12 and C14A-T8. Coloured arrows indicate magnitude and direction of flow. **(D)** Grey shading indicates differences of flow magnitude between **B** and **C** (see key). Changes in flow direction are small (see Supplementary Fig.3). See Materials and Methods for time classes, and main text for further details.

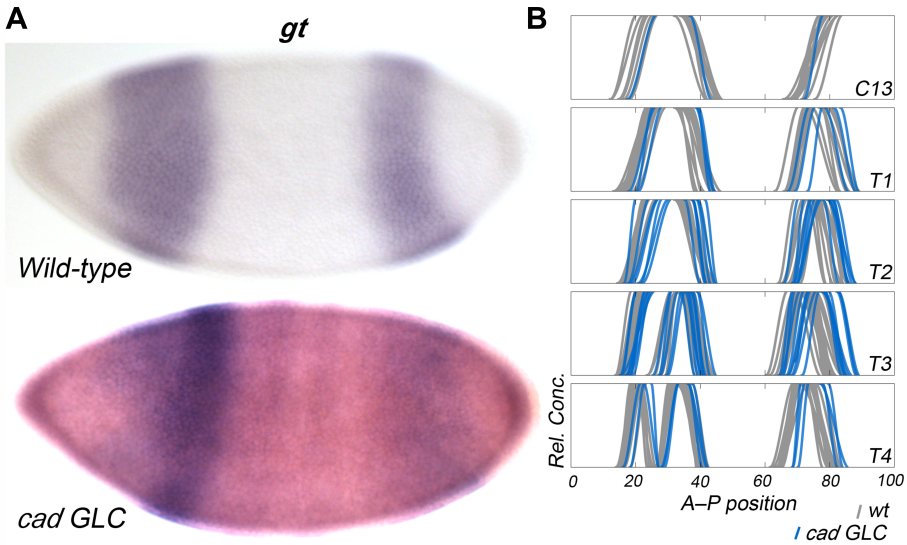

Figure 5: **Shifts of the posterior *gt* domain are delayed in embryos lacking maternal caudal. (A)** Expression of *gt* at T2 in wild-type and *cad* germ-line clone (*cad* GLC) embryos lacking only maternal cad (purple stain: *gt*, weak red stain: *even-skipped*). Embryo images show lateral views: anterior is to the left, dorsal is up. **(B)** Summary graphs comparing wild-type boundary positions (grey) to boundary positions in *cad* GLC embryos (blue coloured lines) from time points C13 to C14-T4. Posterior *gt* domain boundaries begin at positions identical to wild-type. As development progresses these boundaries are consistently placed more posterior in *cad* germ-line clones than in wild-type embryos, indicating delayed anterior shifts in the mutants.

decrease (and thus the magnitude of the difference between Cad levels in both simulations also decreases), differences are more subtle (Fig. 4B–D, time class T8). The altered early flow explains the slower initial build-up of Kr and Kni at low Cad, while later shift dynamics are similar, independent of Cad level. As a result of the altered early flow, the "radius" of the spiral trajectories decreases as Cad concentration is reduced. Counterintuitively, progress along these tightened spirals is much slower than in simulations with wild-type levels of Cad due to weaker flow in regions of phase space near the origin (compare Supplementary Figs. 2 and 4). Slow progress means a delayed switch from the Kr-Kni to the Kni-Gt plane, which results in the decrease in shift velocity for the Kr-Gt interface shown in Fig. 4A.

Discussion

In this paper, we show that a damped oscillator mechanism—with excitable, relaxation-like behaviour—can explain robust segmental patterning of the long-germband insect *D. melanogaster*. Even though they are not periodic, kinematic shifts of gap gene expression domains in our model are an emergent property of temporally regulated gene expression driven by an oscillatory mechanism. In this sense, they are equivalent to the travelling waves of gene expression involved in vertebrate somitogenesis [50, 48] and short-germband arthropod segmentation [6, 61, 18, 4, 19]. This lends support to the notion that regulatory dynamics of segmentation gene expression in long- and short-germband insects are much more similar than is evident at first sight [68].

While oscillatory mechanisms are involved in both long- and short-germband segmentation, it is important to stress that the factors constituting each particular regulatory system are different. Shifting gap domains play a central role in segmental patterning in *D. melanogaster* by directly regulating stripes of pair-rule gene expression. Posterior pair-rule stripes also exhibit anterior shifts in this species, which are produced by, and closely reflect, the expression dynamics of the gap-gene damped oscillator [67]. In contrast, gap genes play a much less prominent role in patterning posterior segments in short-germband arthropods. Instead, periodic kinematic waves of pair-rule gene expression are thought to be generated by negative feedback between the pair-rule genes themselves (in *T. castaneum*, [7]), or by an intercellular oscillator driven by Notch/Delta signalling (in cockroaches, [57], and centipedes, [6, 4]).

The evolutionary transition from short- to long-germband segmentation must have involved the recruitment of gap genes for pair-rule gene regulation, to replace the ancestral oscillatory mechanism [52, 54, 53, 28, 63]. The mechanistic details of how this occurred remain unclear. Traditionally, long- and short-germband modes of patterning have been assumed to be mutually exclusive in any given region of the embryo. In contrast, our results suggest that the replacement process could have occurred gradually, gap- and pair-rule oscillators coexisting temporarily, which would greatly facilitate the transition. In this scenario, gap genes "take over" pair-rule driven oscillatory patterning in the posterior, and later convert to a more switch-like static patterning mode, as observed in the anterior of the *D. melanogaster* embryo [29, 67, 40, 72]. This is tentatively supported by the fact that the spatial extent of the posterior region, which is patterned by shifting gap domains, differs between dipteran species [23, 78].

Seen from another angle, our results imply that equivalent regulatory dynamics (travelling waves of gene expression) can be produced by different oscillatory mechanisms. The use of divergent regulatory mechanisms to independently pattern identical expression domains appears to be very common (see, for example, [21, 55, 22, 5]). Indeed, the relative contribution of different mechanisms may evolve over time, with little effect on downstream patterning [80]. This type of compensatory evolution is called developmental system drift [74, 69, 73, 26, 51]. It has recently been shown to occur extensively in the evolution of the dipteran

gap gene system [78, 15]. System drift provides the necessary conditions that enable the facilitated gradual transition between the different regulatory mechanisms described above.

Even though the core mechanisms that generate oscillatory behaviour differ, some aspects of segmentation gene regulation are strikingly similar between long- and short-germband insects. In both *D. melanogaster* and *T. castaneum*, the speed at which gene expression waves travel through the tissue are positively correlated with the concentration of Cad in the posterior of the embryo (our results and [19, 78, 72]). Cad also appears to control temporal aspects of pair-rule gene regulation in centipedes [6, 4]). From this, we conclude that the role of Cad in regulating oscillatory dynamics is highly conserved. While Cad acts at the level of the pair-rule genes in centipedes and *T. castaneum*, it exerts its effect primarily through regulating gap domain shifts in *D. melanogaster*. Interestingly, even in this long-germband insect, Cad has been shown to retain direct regulation of pair-rule gene expression [39, 36, 27, 17, 43, 49]. This is even more pronounced in the scuttle fly *Megaselia abdita* (also a long-germband insect), where the main effect of Cad on pattern formation remains at the level of the pair-rule genes [79]. This provides further evidence for the recruitment of gap genes into a conserved segmental regulatory cascade involving Cad-mediated regulation of oscillatory pair-rule dynamics.

Our insights into the role of Cad in regulating the gap-gene damped oscillator have further implications. Travelling waves of gene expression that narrow and slow down over time are involved in both arthropod segmentation and vertebrate somitogenesis. It has long been recognised that these expression dynamics imply differential regulation of the rate of an oscillatory process along the A–P axis [50]. However, mechanistic explanations for this phenomenon remain elusive. A number of recent models simply assume that the concentration of some posterior morphogen determines the period of cellular oscillators, without investigating how this might arise (see, for example, [24, 42, 19]). Experimental evidence from vertebrates suggests alteration of protein stability or translational time delays as a possible mechanism [3, 62]. In contrast, our dynamical analysis illustrates how slowing (damped) oscillations can emerge directly from the intrinsic regulatory dynamics of a transcriptional network, without altering rates of protein synthesis or turnover. A similar mechanism, based on intrinsic oscillatory dynamics of a gene network, was recently proposed for vertebrate somitogenesis [11]. It will be interesting to investigate which specific regulatory interactions mediate the effect of Cad on the *T. castaneum* pair-rule gene oscillator.

In summary, we argue that oscillatory mechanisms of gene regulation are not exclusive to short-germband segmentation or somitogenesis. Our analysis provides evidence that the spatial pattern of gap gene expression in the posterior region of the *D. melanogaster* embryo also emerges from a temporal sequence of gap gene expression driven by oscillatory dynamics. This results in the observed anterior shifts of posterior gap domains. We suggest that the dynamic nature of posterior gap gene patterning is a consequence of the context in which it evolved, and that two different oscillatory mechanisms may have coexisted during the transition from short- to long-germband segmentation. Studies using genetics

and data-driven modelling in non-model organisms will reveal the regulatory circuits responsible for driving the different dynamics involved in segmentation processes, as well as the precise nature of the regulatory changes involved in transitions between them [13, 78, 15]. Given the insights gained through its application to gap gene patterning in *D. melanogaster*, phase space analysis will provide a suitable dynamic regulatory context in which to interpret and analyse these results.

Materials and Methods

The gene circuit model

The gap gene circuit model used for our analysis consists of a one-dimensional row of nuclei along the A–P axis. Continuous dynamics during interphase alternate with discrete nuclear divisions. Our analysis includes the segmented trunk region of the embryo between 35 and 73% A–P position. We model the last two cleavage cycles of the blastoderm stage (C13 and C14A) up to the onset of gastrulation; C14A is subdivided into eight equally spaced time classes (T1–T8). Division occurs at the end of C13.

The state variables of the system represent the concentrations of proteins encoded by gap genes *hb*, *Kr*, *gt*, and *kni*. The concentration of protein a in nucleus i at time t is given by $g_i^a(t)$. Change in protein concentration over time occurs according to the following system of ordinary differential equations:

$$\frac{dg_i^a(t)}{dt} = R^a \phi(u^a) - \lambda^a g_i^a(t) \tag{1}$$

where R^a and λ^a are rates of protein production and decay, respectively. ϕ is a sigmoid regulation-expression function used to represent the saturating, coarse-grained kinetics of transcriptional regulation. It is defined as

$$\phi(u^a) = \frac{1}{2}\left(\frac{u^a}{\sqrt{(u^a)^2+1}} + 1\right) \tag{2}$$

where

$$u^a = \sum_{b\in G} W^{ba} g_i^a(t) + \sum_{m\in M} E^{ma} g_i^m(t) + h^a \tag{3}$$

The set of trunk gap genes is given by $G = \{hb, Kr, gt, kni\}$, and the set of external (maternal) regulatory inputs by $M = \{\mathrm{Bcd}, \mathrm{Cad}\}$. Concentrations of maternal regulators g_i^m are interpolated from quantified spatio-temporal protein expression data [67, 56, 2]. Changing maternal protein concentrations means that parameter term $\sum_{m\in M} E^{ma} g_i^m(t)$ is time-dependent, which renders the model non-autonomous.

Interconnectivity matrices W and E represent regulatory interactions between gap genes, and from external maternal inputs, respectively. Matrix elements w^{ba} and e^{ma} are regulatory weights. They summarize the effect of

regulator b or m on target gene a, and can be positive (representing an activation), negative (repression), or near zero (no interaction). h^a is a threshold parameter representing the basal activity of gene a, which includes the effects of regulatory inputs from spatially uniform regulators in the early embryo. The system of equations (1) governs regulatory dynamics during interphase; R^a is set to zero during mitosis.

Model fitting and selection

We obtain values for parameters R^a, λ^a, W, E, and h^a by fitting the model to data [58, 34, 2, 14]. Details of model fitting and selection of solutions are described in the Supplementary Information. Briefly: model equations (1) are solved numerically, and the resulting model output is compared to a quantitative data set of spatio-temporal gap protein profiles. The difference between model output and data is minimized using parallel Lam Simulated Annealing (pLSA). Model fitting was performed on the Mare Nostrum cluster at the Barcelona Supercomputing Centre (http://www.bsc.es). The best-fitting solution was selected for further analysis as described in the Supplementary Information. The resulting diffusion-less, non-autonomous gene circuit accurately reproduces gap gene expression (Fig.1A).

Model analysis

We use a graphical approach [64] to characterise time-variable phase space geometry in a non-autonomous gap gene circuit as previously described in [71]. Briefly: we generate instantaneous phase portraits [8, 71] for each nucleus at 10 time points: C13, C14A/T1–8, and gastrulation time; this is achieved by keeping all time-dependent parameter values constant at each time point. We then calculate the position of steady states in phase space, and classify them into saddles and attractors (including spiral sinks) by eigenvalue analysis to determine their stability [64]. Since nuclei express a maximum of three trunk gap genes over the developmental time covered by our model, we can visualise phase space geometry (attractors, their basins, and the flow of the system) by two- or three-dimensional projections of the four-dimensional phase portrait. See Supplementary Information for details.

Experimental Methodology

Embryos from *cad* mutant germ-line clones were generated and collected as previously described [78]. mRNA expression patterns of the gap genes *gt* or *kni*, and the pair-rule gene *even-skipped (eve)* were visualised using an established enzymatic (colorimetric) *in situ* hybridization protocol [14]. Images were taken and processed to extract the position of expression domain boundaries as described in [12].

Acknowledgments

We would like to acknowledge Nick Monk for countless discussions and help with the analysis of non-autonomous gene circuits. We thank Anna Kicheva for critical reading and comments that significantly improved our initial drafts of this paper. James Sharpe, Jordi García-Ojalvo, Astrid Hoermann, Barbara Negre, Damjan Cicin-Sain and Alba Jiménez-Asins provided guidance and intellectual stimulation during this project. The authors thankfully acknowledge the computer resources, technical expertise and assistance provided by the Barcelona Supercomputing Center—Centro Nacional de Supercomputación. BV was supported by a "la Caixa" fellowship, and a Writing-up Fellowship at the KLI Klosterneuburg. The research group of JJ was supported by the MEC-EMBL agreement for the EMBL/CRG Research Unit in Systems Biology, European Commission grant FP7-KBBE-2011-5/289434 (BioPreDyn), and grants BFU2009-10184 and BFU2012-33775 from MINECO. JJ thanks the Wissenschaftskolleg zu Berlin (Wiko) for a 10-month fellowship in 2014/15. The Centre for Genomic Regulation (CRG) acknowledges support from MINECO, "Centro de Excelencia Severo Ochoa 2013- 2017," SEV-2012-0208.

References

[1] M. Akam. The molecular basis for metameric pattern in the drosophila embryo. *Development*, 101(1):1–22, 1987.

[2] M. Ashyraliyev, K. Siggens, H. Janssens, J. Blom, M. Akam, and J. Jaeger. Gene circuit analysis of the terminal gap gene huckebein. *PLoS Comput Biol*, 5(10):e1000696, 2009.

[3] A. Ay, J. Holland, A. Sperlea, G. S. Devakanmalai, S. Knierer, S. Sangervasi, A. Stevenson, and E. M. Özbudak. Spatial gradients of protein-level time delays set the pace of the traveling segmentation clock waves. *Development*, 141(21):4158–4167, 2014.

[4] C. Brena and M. Akam. An analysis of segmentation dynamics throughout embryogenesis in the centipede strigamia maritima. *BMC biology*, 11(1):1, 2013.

[5] E. Cannavò, P. Khoueiry, D. A. Garfield, P. Geeleher, T. Zichner, E. H. Gustafson, L. Ciglar, J. O. Korbel, and E. E. Furlong. Shadow enhancers are pervasive features of developmental regulatory networks. *Current Biology*, 26(1):38–51, 2016.

[6] A. D. Chipman, W. Arthur, and M. Akam. A double segment periodicity underlies segment generation in centipede development. *Current Biology*, 14(14):1250–1255, 2004.

[7] C. P. Choe, S. C. Miller, and S. J. Brown. A pair-rule gene circuit defines segments sequentially in the short-germ insect tribolium castaneum. *Proceedings of the National Academy of Sciences*, 103(17):6560–6564, 2006.

[8] J. R. Collier, N. A. Monk, P. K. Maini, and J. H. Lewis. Pattern formation by lateral inhibition with feedback: a mathematical model of delta-notch intercellular signalling. *Journal of Theoretical Biology*, 183(4):429–446, 1996.

[9] J. Cooke and E. C. Zeeman. A clock and wavefront model for control of the number of repeated structures during animal morphogenesis. *Journal of theoretical biology*, 58(2):455–476, 1976.

[10] F. Corson and E. D. Siggia. Geometry, epistasis, and developmental patterning. *Proceedings of the National Academy of Sciences*, 109(15):5568–5575, 2012.

[11] J. Cotterell, A. Robert-Moreno, and J. Sharpe. A local, self-organizing reaction-diffusion model can explain somite patterning in embryos. *Cell systems*, 1(4):257–269, 2015.

[12] A. Crombach, D. Cicin-Sain, K. R. Wotton, and J. Jaeger. Medium-throughput processing of whole mount in situ hybridisation experiments into gene expression domains. *PLoS One*, 7(9):e46658, 2012.

[13] A. Crombach, M. A. García-Solache, and J. Jaeger. Evolution of early development in dipterans: reverse-engineering the gap gene network in the moth midge clogmia albipunctata (psychodidae). *Biosystems*, 123:74–85, 2014.

[14] A. Crombach, K. R. Wotton, D. Cicin-Sain, M. Ashyraliyev, and J. Jaeger. Efficient reverse-engineering of a developmental gene regulatory network. *PLoS Comput Biol*, 8(7):e1002589–e1002589, 2012.

[15] A. Crombach, K. R. Wotton, E. Jimenez-Guri, and J. Jaeger. Gap gene regulatory dynamics evolve along a genotype network. *Molecular Biology and Evolution*, 33(5):1293–1307, 2016.

[16] G. K. Davis and N. H. Patel. Short, long, and beyond: molecular and embryological approaches to insect segmentation. *Annual review of entomology*, 47(1):669–699, 2002.

[17] C. R. Dearolf, J. Topol, and C. S. Parker. The caudal gene product is a direct activator of fushi tarazu transcription during drosophila embryogenesis. *Nature*, 1989.

[18] E. El-Sherif, M. Averof, and S. J. Brown. A segmentation clock operating in blastoderm and germband stages of tribolium development. *Development*, 139(23):4341–4346, 2012.

[19] E. El-Sherif, X. Zhu, J. Fu, and S. J. Brown. Caudal regulates the spatiotemporal dynamics of pair-rule waves in tribolium. *PLoS Genet*, 10(10):e1004677, 2014.

[20] P. Francois and E. D. Siggia. Phenotypic models of evolution and development: geometry as destiny. *Current opinion in genetics & development*, 22(6):627–633, 2012.

[21] N. Frankel, G. K. Davis, D. Vargas, S. Wang, F. Payre, and D. L. Stern. Phenotypic robustness conferred by apparently redundant transcriptional enhancers. *Nature*, 466(7305):490–493, 2010.

[22] M. Fujioka and J. B. Jaynes. Regulation of a duplicated locus: Drosophila sloppy paired is replete with functionally overlapping enhancers. *Developmental biology*, 362(2):309–319, 2012.

[23] M. García-Solache, J. Jaeger, and M. Akam. A systematic analysis of the gap gene system in the moth midge clogmia albipunctata. *Developmental biology*, 344(1):306–318, 2010.

[24] F. Giudicelli, E. M. Özbudak, G. J. Wright, and J. Lewis. Setting the tempo in development: an investigation of the zebrafish somite clock mechanism. *PLoS Biol*, 5(6):e150, 2007.

[25] V. V. Gursky, L. Panok, E. M. Myasnikova, M. G. Samsonova, J. Reinitz, A. M. Samsonov, et al. Mechanisms of gap gene expression canalization in the drosophila blastoderm. *BMC systems biology*, 5(1):118, 2011.

[26] E. S. Haag. Compensatory vs. pseudocompensatory evolution in molecular and developmental interactions. *Genetica*, 129(1):45–55, 2007.

[27] T. Häder, A. La Rosée, U. Ziebold, M. Busch, H. Taubert, H. Jäckle, and R. Rivera-Pomar. Activation of posterior pair-rule stripe expression in response to maternal caudal and zygotic knirps activities. *Mechanisms of development*, 71(1):177–186, 1998.

[28] J. Jaeger. The gap gene network. *Cellular and Molecular Life Sciences*, 68(2):243–274, 2011.

[29] J. Jaeger, M. Blagov, D. Kosman, K. N. Kozlov, E. Myasnikova, S. Surkova, C. E. Vanario-Alonso, M. Samsonova, D. H. Sharp, J. Reinitz, et al. Dynamical analysis of regulatory interactions in the gap gene system of drosophila melanogaster. *Genetics*, 167(4):1721–1737, 2004.

[30] J. Jaeger, D. Irons, and N. Monk. Regulative feedback in pattern formation: towards a general relativistic theory of positional information. *Development*, 135(19):3175–3183, 2008.

[31] J. Jaeger, D. Irons, and N. Monk. The inheritance of process: a dynamical systems approach. *Journal of Experimental Zoology Part B: Molecular and Developmental Evolution*, 318(8):591–612, 2012.

[32] J. Jaeger and N. Monk. Bioattractors: dynamical systems theory and the evolution of regulatory processes. *The Journal of physiology*, 592(11):2267–2281, 2014.

[33] J. Jaeger and J. Reinitz. On the dynamic nature of positional information. *BioEssays*, 28(11):1102–1111, 2006.

[34] J. Jaeger, S. Surkova, M. Blagov, H. Janssens, D. Kosman, K. N. Kozlov, et al. Dynamic control of positional information in the early drosophila embryo. *Nature*, 430(6997):368–371, 2004.

[35] S. V. Keränen, C. C. Fowlkes, C. L. L. Hendriks, D. Sudar, D. W. Knowles, J. Malik, and M. D. Biggin. Three-dimensional morphology and gene expression in the drosophila blastoderm at cellular resolution ii: dynamics. *Genome biology*, 7(12):R124, 2006.

[36] A. La Rosée, T. Häder, H. Taubert, R. Rivera-Pomar, and H. Jäckle. Mechanism and bicoid-dependent control of hairy stripe 7 expression in the posterior region of the drosophila embryo. *The EMBO journal*, 16(14):4403–4411, 1997.

[37] P. Z. Liu and T. C. Kaufman. Short and long germ segmentation: unanswered questions in the evolution of a developmental mode. *Evolution & development*, 7(6):629–646, 2005.

[38] J. A. Lynch, E. El-Sherif, and S. J. Brown. Comparisons of the embryonic development of drosophila, nasonia, and tribolium. *Wiley Interdisciplinary Reviews: Developmental Biology*, 1(1):16–39, 2012.

[39] P. M. Macdonald, P. Ingham, and G. Struhl. Isolation, structure, and expression of even-skipped: a second pair-rule gene of drosophila containing a homeo box. *Cell*, 47(5):721–734, 1986.

[40] Manu, A. V. Spirov, V. V. Gursky, H. Janssens, A.-R. Kim, O. Radulescu, C. E. Vanario-Alonso, D. H. Sharp, M. Samsonova, and J. Reinitz. Canalization of gene expression and domain shifts in the drosophila blastoderm by dynamical attractors. *PLoS Computational Biology*, 5(3), 2009.

[41] Manu, A. Surkova, A. Spirov, V. Gursky, H. Janssens, A. Kim, O. Radulascu, C. Vanario-Alonso, D. Sharp, M. Samsonova, and J. ReinitzJ. Canalization of gene expression in the drosophila blastoderm by gap gene cross regulation. *Plos Biology*, 7:e1000049, 2009.

[42] L. G. Morelli, S. Ares, L. Herrgen, C. Schröter, F. Jülicher, and A. C. Oates. Delayed coupling theory of vertebrate segmentation. *HFSP journal*, 3(1):55–66, 2009.

[43] E. Moreno and G. Morata. Caudal is the hox gene that specifies the most posterior drosophile segment. *Nature*, 400(6747):873–877, 1999.

[44] A. W. Murray and M. W. Kirschner. Cyclin synthesis drives the early embryonic cell cycle. *Nature*, 339(6222):275–280, 1989.

[45] J. D. Murray. *Mathematical Biology. II Spatial Models and Biomedical Applications* {*Interdisciplinary Applied Mathematics V. 18*}. Springer-Verlag New York Incorporated, 2001.

[46] A. Nakamoto, S. Hester, S. Constantinou, W. Blaine, A. Tewksbury, M. Matei, L. M. Nagy, and T. Williams. Changing cell behaviours during beetle embryogenesis correlates with slowing of segmentation. *Nature communications*, 6, 2015.

[47] B. Novak, P. Vinod, P. Freire, and O. Kapuy. Systems-level feedback in cell-cycle control. *Biochemical Society Transactions*, 38(5):1242–1246, 2010.

[48] A. C. Oates, L. G. Morelli, and S. Ares. Patterning embryos with oscillations: structure, function and dynamics of the vertebrate segmentation clock. *Development*, 139(4):625–639, 2012.

[49] E. C. Olesnicky, A. E. Brent, L. Tonnes, M. Walker, M. A. Pultz, D. Leaf, and C. Desplan. A caudal mrna gradient controls posterior development in the wasp nasonia. *Development*, 133(20):3973–3982, 2006.

[50] I. Palmeirim, D. Henrique, D. Ish-Horowicz, and O. Pourquié. Avian hairy gene expression identifies a molecular clock linked to vertebrate segmentation and somitogenesis. *Cell*, 91(5):639–648, 1997.

[51] M. Pavlicev and G. P. Wagner. A model of developmental evolution: selection, pleiotropy and compensation. *Trends in Ecology & Evolution*, 27(6):316–322, 2012.

[52] A. Peel. The evolution of arthropod segmentation mechanisms. *BioEssays*, 26(10):1108–1116, 2004.

[53] A. D. Peel. The evolution of developmental gene networks: lessons from comparative studies on holometabolous insects. *Philosophical Transactions of the Royal Society of London B: Biological Sciences*, 363(1496):1539–1547, 2008.

[54] A. D. Peel, A. D. Chipman, and M. Akam. Arthropod segmentation: beyond the drosophila paradigm. *Nature Reviews Genetics*, 6(12):905–916, 2005.

[55] M. W. Perry, A. N. Boettiger, and M. Levine. Multiple enhancers ensure precision of gap gene-expression patterns in the drosophila embryo. *Proceedings of the National Academy of Sciences*, 108(33):13570–13575, 2011.

[56] A. Pisarev, E. Poustelnikova, M. Samsonova, and J. Reinitz. Flyex, the quantitative atlas on segmentation gene expression at cellular resolution. *Nucleic acids research*, 37(suppl 1):D560–D566, 2009.

[57] J. Pueyo, R. Lanfear, and J. Couso. Ancestral notch-mediated segmentation revealed in the cockroach periplaneta americana. *Proceedings of the National Academy of Sciences*, 105(43):16614–16619, 2008.

[58] J. Reinitz and D. H. Sharp. Mechanism of eve stripe formation. *Mechanisms of development*, 49(1):133–158, 1995.

[59] M. I. Rosenberg, J. A. Lynch, and C. Desplan. Heads and tails: evolution of antero-posterior patterning in insects. *Biochimica et Biophysica Acta (BBA)-Gene Regulatory Mechanisms*, 1789(4):333–342, 2009.

[60] K. Sander. Specificatio n of the basic body pattern in insect embryogenesis. *Adv. Insect Physiol*, 12:124, 1976.

[61] A. Sarrazin, A. Peel, and M. Averof. A segmentation clock with two-segment periodicity in insects. *Science*, 336:338–341, 2012.

[62] C. Schröter, S. Ares, L. G. Morelli, A. Isakova, K. Hens, D. Soroldoni, M. Gajewski, F. Jülicher, S. J. Maerkl, B. Deplancke, et al. Topology and dynamics of the zebrafish segmentation clock core circuit. *PLoS Biol*, 10(7):e1001364, 2012.

[63] R. Stahi and A. D. Chipman. Blastoderm segmentation in oncopeltus fasciatus and the evolution of insect segmentation mechanisms. *Proc. R. Soc. B*, 283(1840):20161745, 2016.

[64] S. H. Strogatz. *Nonlinear dynamics and chaos: with applications to physics, biology, chemistry, and engineering*. Westview press, Boulder. CO, 2014.

[65] G. Struhl, P. Johnston, and P. A. Lawrence. Control of drosophila body pattern by the hunchback morphogen gradient. *Cell*, 69(2):237–249, 1992.

[66] É. Sucena, K. Vanderberghe, V. Zhurov, and M. Grbić. Reversion of developmental mode in insects: evolution from long germband to short germband in the polyembrionic wasp macrocentrus cingulum brischke. *Evolution & development*, 16(4):233–246, 2014.

[67] S. Surkova, D. Kosman, K. Kozlov, E. Myasnikova, A. A. Samsonova, A. Spirov, C. E. Vanario-Alonso, M. Samsonova, J. Reinitz, et al. Characterization of the drosophila segment determination morphome. *Developmental biology*, 313(2):844–862, 2008.

[68] D. Tautz. Segmentation. *Developmental cell*, 7(3):301–312, 2004.

[69] J. R. True and E. S. Haag. Developmental system drift and flexibility in evolutionary trajectories. *Evolution & development*, 3(2):109–119, 2001.

[70] S. Vakulenko, J. Reinitz, O. Radulescu, et al. Size regulation in the segmentation of drosophila: interacting interfaces between localized domains of gene expression ensure robust spatial patterning. *Physical review letters*, 103(16), 2009.

[71] B. Verd, A. Crombach, and J. Jaeger. Classification of transient behaviours in a time-dependent toggle switch model. *BMC systems biology*, 8(1):43, 2014.

[72] B. Verd, A. Crombach, and J. Jaeger. Dynamic maternal gradients control timing and shift-rates for *drosophila* gap gene expression. *Submitted to PLoS Computational Biology*, 2016.

[73] K. M. Weiss. The phenogenetic logic of life. *Nature Reviews Genetics*, 6(1):36–45, 2005.

[74] K. M. Weiss and S. M. Fullerton. Phenogenetic drift and the evolution of genotype–phenotype relationships. *Theoretical population biology*, 57(3):187–195, 2000.

[75] A. Winfree. The geometry of biological time (section 8d), 1980.

[76] L. Wolpert. The french flag problem: a contribution to the discussion on pattern development and regulation. *Towards a theoretical biology*, 1:125–133, 1968.

[77] L. Wolpert. Positional information and the spatial pattern of cellular differentiation. *Journal of theoretical biology*, 25(1):1–47, 1969.

[78] K. R. Wotton, E. Jiménez-Guri, A. Crombach, H. Janssens, A. Alcaine-Colet, S. Lemke, U. Schmidt-Ott, and J. Jaeger. Quantitative system drift compensates for altered maternal inputs to the gap gene network of the scuttle fly megaselia abdita. *Elife*, 4:e04785, 2015.

[79] K. R. Wotton, E. Jiménez-Guri, and J. Jaeger. Maternal co-ordinate gene regulation and axis polarity in the scuttle fly megaselia abdita. *PLoS Genet*, 11(3):e1005042, 2015.

[80] Z. Wunderlich, M. D. Bragdon, B. J. Vincent, J. A. White, J. Estrada, and A. H. DePace. Krüppel expression levels are maintained through compensatory evolution of shadow enhancers. *Cell reports*, 12(11):1740–1747, 2015.